Syntaxin clusters at secretory granules in a munc18-bound conformation

Peng Yin, Nikhil R. Gandasi, Swati Arora, Muhmmad Omar-Hmeadi, Jan Saras, and Sebastian Barg*
Institute of Medical Cell Biology, Uppsala University, 75123 Uppsala, Sweden

ABSTRACT **Syntaxin (stx)-1 is an integral plasma membrane protein that is crucial for two distinct steps of regulated exocytosis, docking of secretory granules at the plasma membrane and membrane fusion. During docking, stx1 clusters at the granule docking site, together with the S/M protein munc18. Here we determined features of stx1 that contribute to its clustering at granules. In live insulin-secreting cells, stx1 and stx3 (but not stx4 or stx11) accumulated at docked granules, and stx1 (but not stx4) rescued docking in cells expressing botulinum neurotoxin-C. Using a series of stx1 deletion mutants and stx1/4 chimeras, we found that all four helical domains (Ha, Hb, Hc, SNARE) and the short N-terminal peptide contribute to recruitment to granules. However, only the Hc domain confers specificity, and it must be derived from stx1 for recruitment to occur. Point mutations in the Hc or the N-terminal peptide designed to interfere with binding to munc18-1 prevent stx1 from clustering at granules, and a mutant munc18 deficient in binding to stx1 does not cluster at granules. We conclude that stx1 is recruited to the docking site in a munc18-1–bound conformation, providing a rationale for the requirement for both proteins for granule docking.**

Monitoring Editor
Anne Spang
University of Basel

Received: Sep 6, 2017
Revised: Aug 21, 2018
Accepted: Aug 24, 2018

INTRODUCTION

Regulated exocytosis depends on the formation of a complex between three cognate SNARE proteins that bridges the vesicle and plasma membrane and drives their fusion (Sollner *et al.*, 1993; Sutton *et al.*, 1998). In neurons and many endocrine cells, this complex consists of syntaxin-1A (stx1) and SNAP-25 (synaptosomal associated protein 25) at the plasma membrane and VAMP2/synaptobrevin-2 (syb) at the vesicle membrane. Each of the proteins contributes one (stx1, syb) or two (SNAP-25) helical SNARE motifs of 60–70 amino acids to the complex (Weimbs *et al.*, 1997). In addition, stx1 contains an autonomously folded Habc domain that is connected with the SNARE motif through a flexible linker and is composed of three additional α-helices (Ha, Hb, and Hc) flanked by a short N-terminal peptide (Npep). Binding of the Habc domain onto the SNARE domain (Sn) results in an alternative four-helix bundle, which is stabilized by the S/M protein munc18. In this closed conformation, the Habc domain binds into the central cavity of munc18, while the N-peptide binds to a hydrophobic patch on its outside (Dulubova *et al.*, 1999; Misura *et al.*, 2000; Burkhardt *et al.*, 2008). "Open" and "closed" syntaxin are in a dynamic equilibrium (Margittai *et al.*, 2003; Chen *et al.*, 2008; Dawidowski and Cafiso, 2013), and intermediate conformations exist when the protein is in its native lipid-bound environment (Liang *et al.*, 2013). By stabilizing the closed form of syntaxin (Dawidowski and Cafiso, 2013), munc18 may act as a chaperone that prevents premature SNARE complex assembly. The transition to the ternary SNARE complex is facilitated by munc13-dependent opening of syntaxin (Yang *et al.*, 2015), and is thought to proceed via an intermediary "acceptor" complex that contains syntaxin, munc18, and SNAP-25, but not synaptobrevin (Zilly *et al.*, 2006; Jakhanwal *et al.*, 2017). The Sec1p/Munc18 (SM) protein munc18-1 binds to stx1 and acts as template for the correct registry of the nascent 4-helix SNARE bundle (Baker *et al.*, 2015); during the transition it is likely held in place by syntaxin's N-peptide (Rathore *et al.*, 2010; Hu *et al.*, 2011).

Both stx1 and munc18 are also necessary for docking of secretory granules at the plasma membrane, a critical step on the path to release competence (Voets *et al.*, 2001; de Wit *et al.*, 2006; Ohara-Imaizumi *et al.*, 2007). Stx1 forms small clusters in the plasma membrane that are 50–100 nm wide and contain ~50–70 copies of the protein (Lang, 2007; Sieber *et al.*, 2007; Barg *et al.*, 2010; Knowles *et al.*, 2010; Bar-On *et al.*, 2012). These clusters depend

This article was published online ahead of print in MBoC in Press (http://www.molbiolcell.org/cgi/doi/10.1091/mbc.E17-09-0541) on August 29, 2018.

*Address correspondence to: Sebastian Barg (sebastian.barg@mcb.uu.se).

Abbreviations used: BoNT-C, botulinum neurotoxin C; EGFP, enhanced green fluorescent protein; Npep, N-terminal peptide of syntaxin; NPY, neuropeptide Y; SM, Sec1p/Munc18; Sn, SNARE domain; SNAP-25, synaptosomal associated protein 25; Stx, syntaxin; Syb, synaptobrevin; TIRF, total internal reflection microscopy.

on cholesterol (Lang *et al.*, 2001) and polyphosphoinositides (Murray and Tamm, 2009) and are thought to result from a self-assembly process that involves the SNARE motif (Sieber *et al.*, 2006) and electrostatic protein–lipid interactions through a series of arginines near the transmembrane domain (van den Bogaart *et al.*, 2011). A fraction of the stx1 clusters colocalize with docked secretory vesicles (on-granule clusters; Lang *et al.*, 2001; Ohara-Imaizumi *et al.*, 2004; Aoyagi *et al.*, 2005; Barg *et al.*, 2010; Honigmann *et al.*, 2013), where they form de novo when a vesicle contacts the plasma membrane to dock (Gandasi and Barg, 2014). This specific binding of stx1 clusters to secretory granules involves its Habc domain, because removing this domain results in a protein that no longer localizes to docked secretory granules (Barg *et al.*, 2010) Overexpression of the Habc fragment displaces stx1 clusters from insulin granules and prevents successful docking (Gandasi and Barg, 2014). Stx4, which is involved in constitutive secretion, also forms clusters in the plasma membrane, but these are distinct from those of stx1 (Sieber *et al.*, 2006).

Here we have analyzed a series of hybrid and mutant stx's to determine which structural features are required for recruitment of the protein to secretory granules, as well as docking and exocytosis. The data indicate that both the Habc domain and the N-peptide are involved in recruitment and docking, and that two amino acids at the N-terminal end of the Hc domain confer specificity of the interaction. We propose that stx1 is recruited during docking in its munc18-bound conformation.

RESULTS

Syntaxin-1 and -3 associate with docked granules and support docking

To test the specificity of stx recruitment to granules, we expressed enhanced green fluorescent protein (EGFP)-labeled stx isoforms 1, 3, 4, and 11 together with the granule marker NPY-mCherry in insulin-secreting INS1 cells. All four isoforms are natively expressed in these cells and in human islets (Kutlu *et al.*, 2009; Gandasi *et al.*, 2018). Docked granules were imaged by TIRF microscopy (Figure 1, a and b), which limits illumination to within about one granule diameter from the plasma membrane. With the exception of stx11, all stx isoforms formed clusters at the plasma membrane. Clusters of stx1 and stx3, but not those of stx4, often overlapped with the positions of docked granules. We quantified this colocalization in two complimentary ways. First, we averaged a large number of images of the stx channel, each centered at the site of a docked granule (Figure 1c). The presence of a central spot in these average images indicated that both stx1 and stx3 were specifically recruited to granule docking sites. In contrast, only weak (stx4) or no (stx11) association was seen with the other isoforms tested. Colocalization with granules was also quantified by image analysis. We determined the amount of stx-EGFP fluorescence specifically associated with the granule (ΔF), normalized by the amount of fluorescence present in a surrounding area that did not contain a granule (S; Barg *et al.*, 2010; Gandasi and Barg, 2014). The resultant quotient is proportional to the apparent affinity of the protein to the granule docking site (Barg *et al.*, 2010). Stx1 and stx3 yielded $\Delta F/S$ values around 0.12, while those of stx4 and stx11 were four to five times lower (Figure 1d). Thus, stx1 and stx3 are strongly recruited to the docking site, while stx4 and stx11 are not.

To test the role of the stx clusters in granule docking, we coexpressed botulinum neurotoxin C (BoNT-C), which specifically cleaves stx1 and stx3 near the C-terminus (Schiavo *et al.*, 1995). Since this removes the Habc domain, we expected that syntaxin would no longer localize to granules. Indeed, BoNT-C expression resulted in uniform distribution of coexpressed stx1-EGFP (Figure 1b), and negligible association of the protein with docked granules (Figure 1, c and d). Docked granules were strongly reduced in BoNT-C–expressing cells, suggesting that endogenous stx isoforms required for docking were cleaved by BoNT-C. Granule docking was

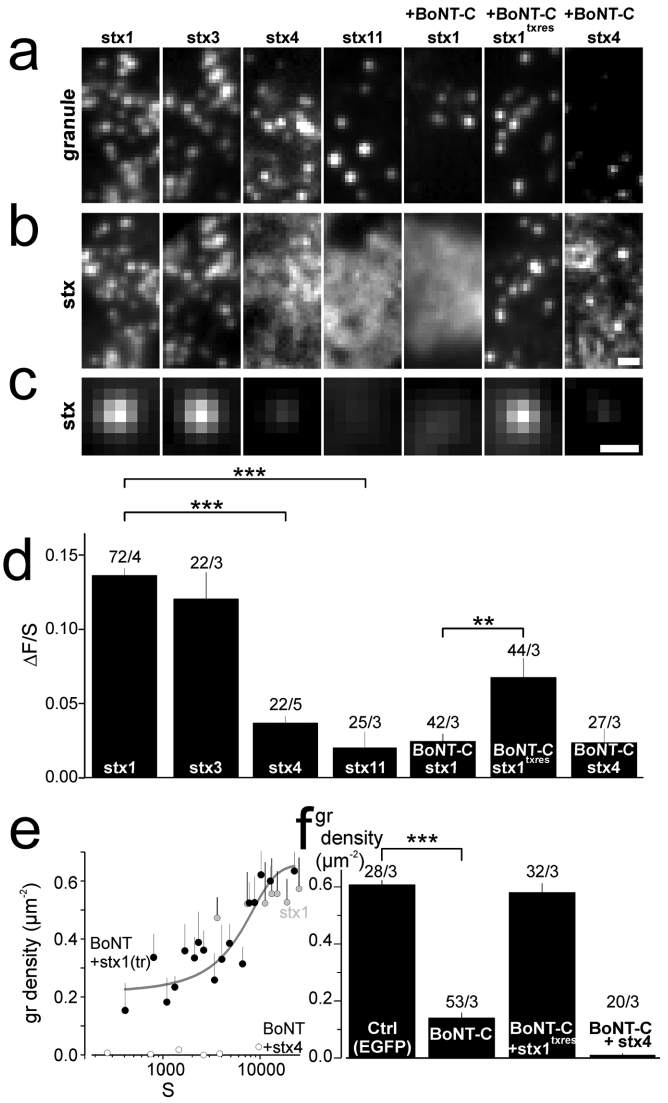

FIGURE 1: The Stx1 N-terminal is crucial for cluster formation at the granule docking sites. (a, b) Representative images showing NPY-mCherry–labeled granules with EGFP-labeled stx variants stx1, stx3, stx4, stx11, stx1 + BoNT-C, stx1^{txrres} + BoNT-C, and stx4 + BoNT-C. BoNT-C was coexpressed with NPY-mCherry using a bicistronic plasmid. Scale bar, 1 μm. (c) Average images of the EGFP channel spatially aligned to granule locations for conditions specified in a and b. Scale bar, 0.5 μm. (d) Quantification of syntaxin binding to the docking site ($\Delta F/S$) for cells in c. Numbers of cells and experiments are given above the bars (cells/experiments). Asterisks indicate statistical significance (**, $p < 0.01$; ***, $p < 0.001$; *t* test). (e) Granule density as function of expression level of EGFP-labeled stx1 (gray circles), stx1^{txres} + BoNT-C (black circles), or stx4 + BoNT-C (white circles). Expression is measured as background-subtracted average EGFP fluorescence in the cell (S). Each data point represents the average (±SEM) of three cells. The yellow line is a Hill function fitted to the green data points. (f) Average granule density for cells shown in e. Numbers of cells and experiments are given above the bars (cells/experiments; ***, $p < 0.001$; *t* test).

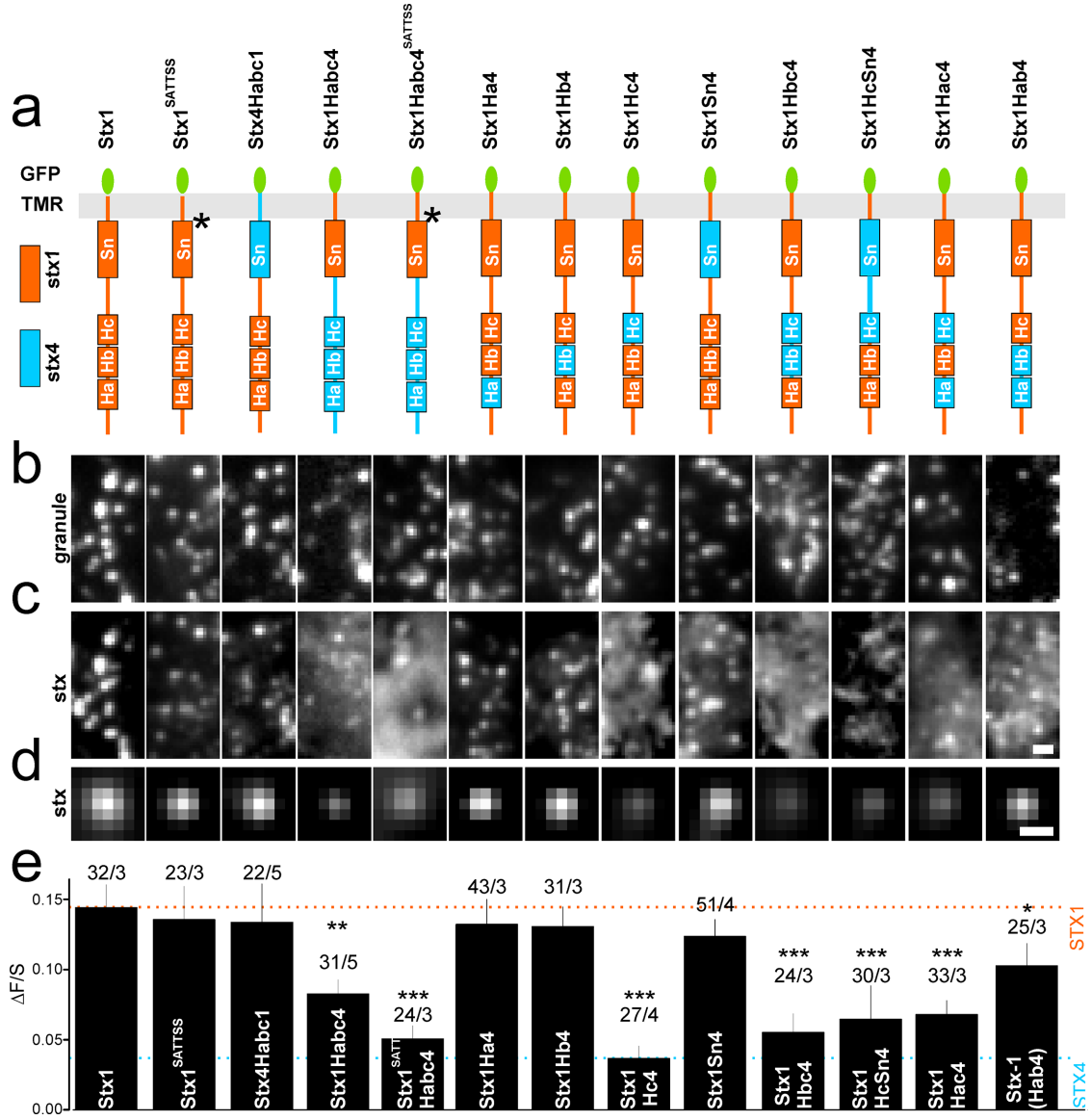

FIGURE 2: The Hc domain is required for the recruitment of stx1 to granules. (a) Cartoons showing chimeric stx1/4 constructs. Point mutations are marked with stars. (b, c) Representative images showing NPY-mCherry–labeled granules with EGFP-labeled stx chimeric constructs stx1^{SATTSS}, stx4Habc1, stx1Habc4, stx1Habc4^{SATTSS}, stx1Ha4, stx1Hb4, stx1Hc4, stx1Sn4, stx1Hbc4, stx1HcSn4, stx1Hac4, and stx1Hab4. (d) Average images of the EGFP channel, c, spatially aligned to granule locations for experiments in b and c. Scale bar, 0.5 µm. (e) Quantification of syntaxin binding to the docking site ($\Delta F/S$) for cells in d. Lines indicate the $\Delta F/S$ values for stx1 (orange) and stx4 (blue) from Figure 1d, for comparison. Numbers of cells and experiments are given above the bars (cells/experiments). Asterisks indicate significant changes from stx1 (*, $p < 0.05$; **, $p < 0.01$; ***, $p < 0.001$; analysis of variance [ANOVA]).

efficiently and dose-dependently rescued by coexpression of toxin-resistant syntaxin-1 (stx1^{txres}), which also associated with docked granules (Figure 1, e and f). In contrast, stx4-EGFP expression did not rescue docking.

Clustering at granules requires the Hc domain of stx1

Next, we created EGFP-labeled hybrid constructs of stx1 and stx4 to study which domains confer the ability of recruitment on granules (Figure 2). Replacing the Habc domain of stx4 (blue in Figure 2a) with that of stx1 (orange in Figure 2a) yielded a protein (termed stx4Habc1) that was efficiently recruited to granules and had $\Delta F/S$ values similar to that of stx1 (Figure 2, b–e). In contrast, when the Habc domain of stx4 was introduced into stx1, $\Delta F/S$ was reduced by half, compared with wild-type (wt) stx1. This protein (stx1Habc4) associated somewhat more strongly with docked granules than wt stx4, suggesting that interactions other than those through the Habc domain must exist. Stx1 aggregates in part through oligomerization that depends on positive charges in its transmembrane domain (van den Bogaart *et al.*, 2011; Honigmann *et al.*, 2013). When these charged amino acids in stx1Habc4 were replaced with neutral amino acids (here referred to as SATTSS, aa 260–265), association of the resultant protein with granules was similar to that for stx4. In contrast, no reduction in the $\Delta F/S$ value was observed when SATTSS was introduced into wt stx1. Next, we tested hybrids in which individual stx1 helices (Ha, Hb, Hc, Sn) were replaced with the analogous stx4 helices. Strikingly, only hybrids in which the Hc helix was

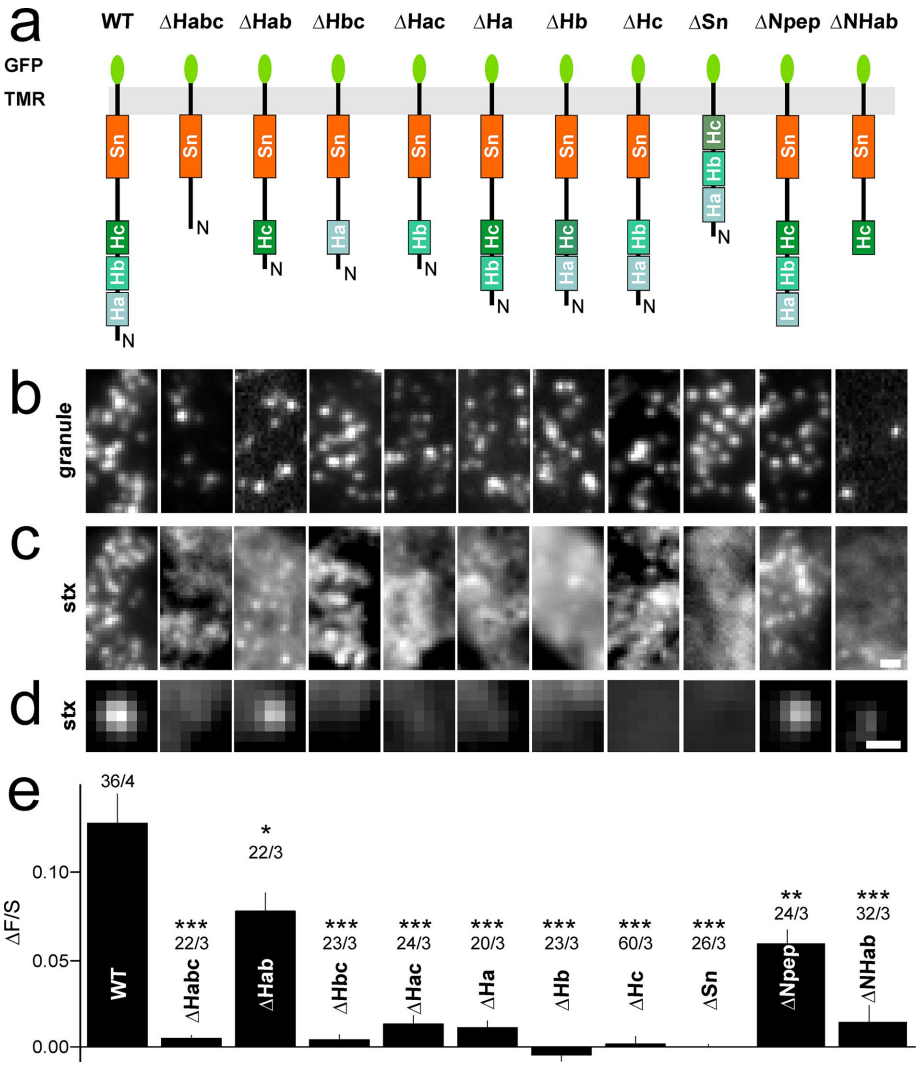

FIGURE 3: Helical domains and the N-terminal peptide are involved in clustering of stx1 at the docking site. (a) Cartoons showing stx1 constructs with deleted domains. (b, c) Representative images showing NPY-mCherry–labeled granules with EGFP-labeled stx constructs stx1 WT (duplicated from Figure 1), stx1ΔHabc, stx1ΔHab, stx1ΔHbc, stx1ΔHac, stx1ΔHa, stx1ΔHb, stx1ΔHc, stx1ΔSn, stx1ΔNpep, and stx1ΔNHab. (d) Average images of the EGFP channel spatially aligned to granule locations for constructs specified in a. Scale bar, 0.5 µm. (e) Quantification of syntaxin binding to the docking site (ΔF/*S*) for cells in d. Numbers of cells and experiments are given above the bars (cells/experiments). Asterisks indicate significant changes from stx1 (*, $p < 0.05$; **, $p < 0.01$; ***, $p < 0.001$; ANOVA).

derived from stx1 were recruited to docked granules more efficiently than stx4 (Figure 2, a–e), while those with Hc derived from stx4 had Δ*F/S* values similar to that of wt stx4 (cf. Figure 1d, dashed blue line in Figure 2e). Replacing the Ha or Hb domains of stx1 with those of stx4 had no effect on its recruitment, and replacement of both Ha and Hb, or of the SNARE domain (Sn), led to a minor reduction. Thus, the Hc domain contains specific features that are required for the recruitment of stx1 to granules, while the three other helical domains can be replaced with those of another stx isoform.

Four helical domains and the N-peptide are required for granule association

Removing the N-terminal Habc domain from stx1 strongly reduces its binding to the docking site (Barg *et al.*, 2010). We studied this effect in more detail and prepared a series of deletion mutants of EGFP-labeled stx1 in which one or more of the four helices Ha, Hb, Hc, or Sn were missing, while retaining the N-peptide (Npep, aa 1–27; see Figure 3a). Deletion of each of the helical domains alone, and most combinations of double deletions, abolished association of the resultant proteins with granules (Figure 3, b–e). However, a stx1 in which both Ha and Hb were deleted (termed ΔHab) was still recruited to granules, although only about half as efficiently as wt stx1. Stx1 with the N-peptide deleted (stx1ΔNpep) was recruited to granules less than half as efficiently as wt stx1. Interestingly, when the N-peptide was deleted from the truncated stx1ΔHab, association with granules was abolished altogether (Figure 3, b–e). The data indicate that all four helical domains and the N-terminal peptide are required for clustering of stx1 at granules, which is consistent with the notion that stx1 is recruited in a conformation that at least partially resembles the closed conformation.

Munc18 is required for recruitment of stx1 to granules

Munc18-1 is required for docking (Voets *et al.*, 2001) and stabilizes the closed conformation of stx1 by binding the coiled-coil Habc bundle into its central cavity (Dulubova *et al.*, 1999; Misura *et al.*, 2000; Dawidowski and Cafiso, 2013). An additional site exists of interaction with the stx1's N-peptide, which is important during SNARE complex assembly (Shen *et al.*, 2010). We therefore tested whether interfering with either of these binding modes would affect recruitment of stx1 to granules or granule docking. An EGFP-labeled stx1 carrying mutations known to prevent binding to the central cavity of munc18-1 (D231A/E234A/N236A/D242A, stx1^{DEND}) (Shi *et al.*, 2011) associated two- to threefold more weakly with docked granules than wildtype stx1 (Figure 4, a–d), suggesting that this binding mode is important for recruitment. On the basis of the crystal structure of munc18-1–bound stx1 (Burkhardt *et al.*, 2008), we created two additional point mutations at the N-terminal end of the Hc-domain to interfere with a hydrophobic interaction between munc18-1 and closed stx1 (Figure 4e). Replacing alanine (A111) and isoleucin (I115) with serines (A111S/I115S, referred to as stx1^{SS}) or with valine and methionine (A111V/I115M, referred to as stx1^{VM}, to resemble stx4) resulted in proteins with strongly reduced ability to cluster at granules. Conversely, when the corresponding residues in stx4 were mutated to AI to resemble stx1 (V118A/M122I, referred to as stx1^{AI}), the resultant protein localized to granules nearly as much as stx1 (Figure 4, a–d).

We confirmed that EGFP-labeled munc18-1 also accumulates at the granule docking site (Pertsinidis *et al.*, 2013; Gandasi and Barg, 2014) and then tested how mutations that interfere with its binding to stx1 affect this recruitment and granule docking (Figure 4, f–i). Mutations in the central cavity of munc18-1 (46E/59K) are well

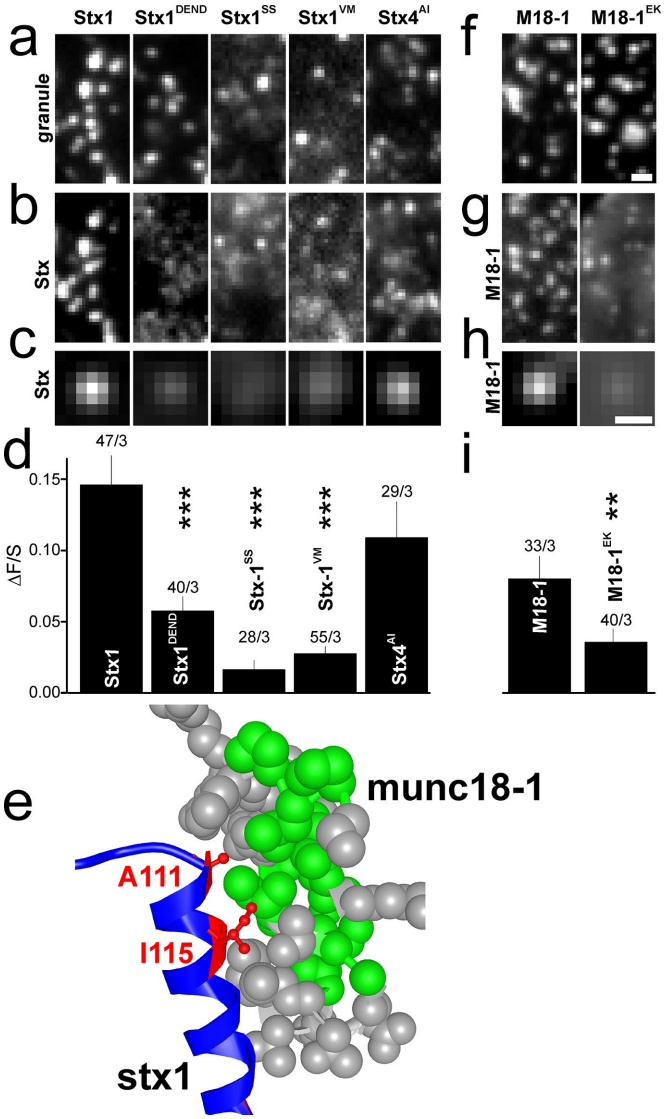

FIGURE 4: Binding of stx1 to munc18-1 is critical for their recruitment to granules. (a, b) Representative images showing NPY-mCherry–labeled granules with EGFP-labeled syntaxin constructs stx1, stx1 D231A/E234A/N236A/D242A (stx1^{DEND}), stx1 A111S/I115S (stx1^{SS}), stx1 A111V/I115M (stx1^{VM}), and stx4 V118A/M122I (stx4^{AI}). (c) Average images of the EGFP channel spatially aligned to granule locations for constructs specified in a and b. Scale bar, 0.5 µm. (d) Quantification of syntaxin binding to the docking site ($\Delta F/S$) for cells in c. Numbers indicate *n* of cells/experiments (***, $p < 0.001$; ANOVA). (e) Cocrystal structure (PDB 3C98) illustrating the interaction between the N-terminal end of the Hc helix of stx1 (blue/red) and munc18-1 (gray/green). Green indicates hydrophobic residues in munc18; red marks stx1 residues A111 and I115 that interact with munc18. (f, g) Representative images showing NPY-mCherry labeled granules with EGFP-labeled munc18 wt or munc18 K46E/E59K (munc18^{EK}). Numbers indicate *n* of cells/experiments (**, $p < 0.01$; ***, $p < 0.001$; ANOVA). (h, i) As in c, d, but for munc18 or munc18^{EK}.

known to prevent its binding to stx1 (Han *et al.*, 2009), and a mutant munc18^{EK}-EGFP had a twofold lower affinity to the docking site than wt munc18-1-EGFP. The data indicate that binding of munc18-1 to stx-1 is critical for recruitment of both proteins to granules. This is consistent with our earlier finding that their time courses of recruitment during docking are very similar (Gandasi and Barg, 2014).

Overexpression of Habc-derived fragments reduces exocytosis in INS1 cells

Expression of soluble Habc fragments competitively displaces stx1 from the granule docking site and reduces both the number of docked granules and exocytosis (Zhou *et al.*, 2013; Gandasi and Barg, 2014). Indeed, expression of an EGFP-tagged Habc fragment of stx1 (aa 1–159) together with the granule marker reduced docked granules by about half (Figure 5b). This was not due to an overall reduced number of granules, because the granule density in confocal images focused at the center of the cell was unchanged (unpublished data). Expression of the individual helical domains Ha, Hb, and Hc (but not Sn) of stx1 decreased docked granules by about one-fourth (Figure 5b). We then tested whether stx1 fragments would affect stimulated exocytosis. Cells coexpressing EGFP-labeled stx1 fragments and the granule marker NPY-mCherry were imaged and individually depolarized by exposure to 75 mM K^+, which resulted in visible exocytosis of a fraction of granules (Figure 5, c and d). In contrast to controls (EGFP), most stx1 fragments partially inhibited exocytosis, with Ha having the strongest inhibitory effect, followed by Hb and Hc. The Sn and the Npep also inhibited exocytosis, although the effects were smaller than with the Habc-derived fragments. Granule priming, which we estimate as the fraction of docked granules that underwent exocytosis, was reduced by expressing Ha, Hb, Hc, and Sn, while the Habc fragment had little or no effect (Figure 5e). We conclude that the presence of the Habc domain fragment affects exocytosis primarily by reducing docked granules, while the SNARE domain fragment mostly affects granule priming. Individually, the Ha, Hb, and Hc domains decrease both docking and priming.

DISCUSSION

Contact of secretory granules with the plasma membrane induces temporally synchronized recruitment of stx1 and munc18, which initiates the formation of a functional release site (Gandasi and Barg, 2014). We show here that this process depends on features in the Habc domain of stx1, and that interaction between stx1 and munc18 is required. At first sight, this is at odds with reports that the SNARE domain, positive charges near the plasma membrane, or the length of the transmembrane domain drive clustering of stx (Sieber *et al.*, 2006; Murray and Tamm, 2011; Milovanovic *et al.*, 2015). However, the various clustering mechanisms of stx1 are not mutually exclusive and likely operate in parallel. Clustering of stx (by self-aggregation or lipid association) and localization of such clusters to granules are separable events, which is consistent with reports that small stx1 clusters coalesce into larger ones (Bar-On *et al.*, 2012) and that the density of stx1 clusters, but not the amount of stx1 bound to granules, increases with the expression level of the protein (Sieber *et al.*, 2006; Barg *et al.*, 2010).

Both the stx1/4 hybrids and the stx1 deletion mutants demonstrate that removal of any one, or of all three helices within the Habc domain prevents accumulation of stx1 at docked granules. This indicates that all four helical domains are required for recruitment of stx1 to docked granules. While this is consistent with a conformation that at least partially resembles the closed stx1 seen in crystal structures (Misura *et al.*, 2000; Burkhardt *et al.*, 2008), it does not exclude intermediates that are partially open (Dawidowski and Cafiso, 2013; Liang *et al.*, 2013). Syntaxin must also be bound by munc18, because mutations that interfere with binding of stx1 to munc18 also prevent clustering of stx1 at granules (Figure 4); this is consistent with earlier findings that most stx1 in the membrane is munc18-1–bound (Schütz *et al.*, 2005; Zilly *et al.*, 2006; Pertsinidis *et al.*, 2013). Moreover, the D34N/M38V mutations near

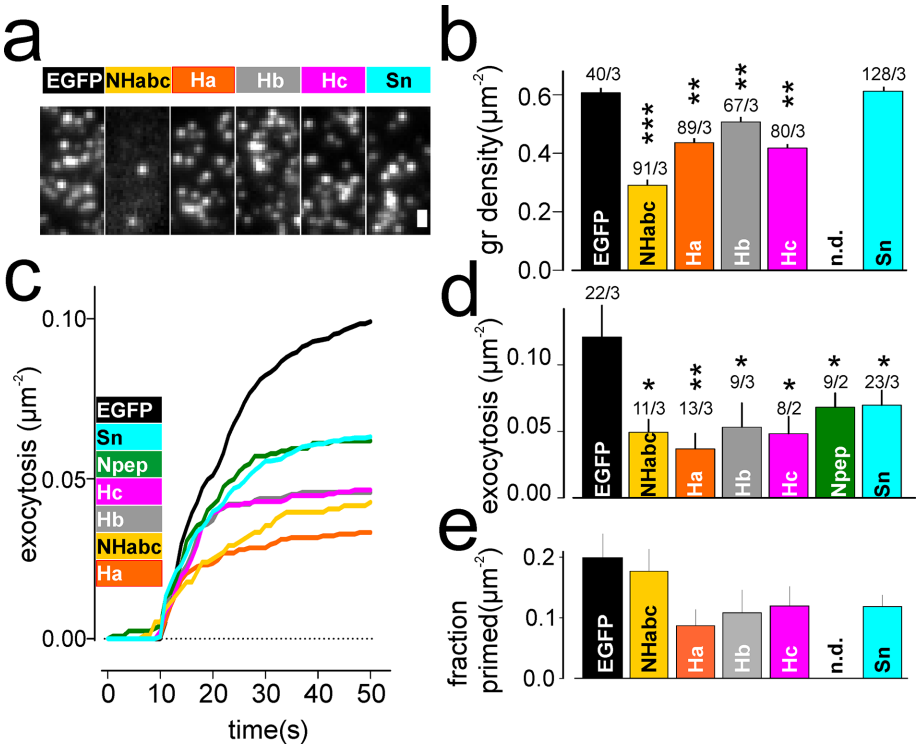

FIGURE 5: Overexpression of Habc helices decreases both docking and exocytosis. (a) Representative images showing NPY-mCherry–labeled granules in cells overexpressing pEGFP or EGFP-labeled Ha, Hb, Hc, SNARE (Sn), and Npep-Habc fragments; scale bar,1 μm. (b) Quantification of granule density in experiments as in a. Numbers indicate *n* of cells/experiments. Asterisks indicate significant difference compared with EGFP (***, $p < 0.001$; **, $p < 0.01$; *t* test). (c) Average cumulative exocytosis events normalized for area in cells stimulated with 75 mM K^+ from $t = 10$ s. Cells expressed EGFP as control (black) or the indicated EGFP-labeled syntaxin fragments. (d) Final exocytosis values in c, normalized for cell footprint area. Numbers indicate *n* of cells/experiments in c and d. Asterisks indicate significant difference compared with EGFP (*, $p < 0.05$; **, $p < 0.01$; *t* test). (e) Fraction of primed granules, obtained by dividing exocytosis values in d with docked granule density in b. SEMs have been calculated using standard error propagation rules; significance was not tested.

the munc18-1 N-terminus, which prevent its binding to closed stx1, strongly affect vesicle docking (Gulyas-Kovacs *et al.*, 2007). In light of these considerations, the relatively strong clustering of the ΔHab is surprising, because it lacks two of the helices.

In the closed conformation of stx1, the Hc domain is located deepest within the central cavity of munc18, adjacent to the SNARE domain, while the remaining Ha and Hb helices are located toward the open face of the cavity (Misura *et al.*, 2000; Burkhardt *et al.*, 2008). Notably, only mutants containing the Hc domain of stx1 associated with docked granules, indicating that specific features within the Hc domain are important for directing stx1 to docked granules. Indeed, we show that two point mutations at the N-terminal end of the Hc (positions A111/I115) can convert stx1 to a phenotype resembling stx4, and vice versa. In contrast, other regions of the protein (Ha, Hb, Sn, N-peptide) could be replaced with those of stx4, which on its own is not strongly recruited to granules. The Hc domain is therefore likely important for determining which stx isoform is present at the release site, and may underlie the fact that SM proteins contribute to SNARE pairing specificity (Peng and Gallwitz, 2002; Shen *et al.*, 2007).

Removal of the N-peptide also weakened accumulation of stx1 at granules, although less than removal of any of the Habc helices. This is consistent with its proposed role in initiating binding between munc18 and stx1 (Rathore *et al.*, 2010) and may explain why the stimulatory action of munc18-1 on exocytosis requires the N-peptide (Shen *et al.*, 2010; Zhou *et al.*, 2013) and why expression of the N-peptide fragment decreases exocytosis (Figure 5d; Park *et al.*, 2016) and blocks neurotransmitter release in the calyx of Held (Khvotchev *et al.*, 2007). The relatively weak effect of N-peptide deletion on clustering is consistent with the finding that a dysfunctional N-peptide reduces exocytosis only when combined with the "constitutively open" LE mutation (Park *et al.*, 2016). Moreover, stx1 lacking the N-peptide can still bind munc18 in a closed conformation (Colbert *et al.*, 2013). Taken together, these results suggest that there is no absolute requirement for the N-peptide during exocytosis or, as we show here, syntaxin recruitment to the release site. In summary, we conclude that stx1 is recruited to the docking site in a munc18-1–bound conformation that depends on the Habc domain and involves specific interactions with the Hc helix. This provides a rationale for the requirement for both proteins during granule docking.

MATERIALS AND METHODS

Cells

INS1-cells clone 832/13 were used throughout this study. Cells were maintained in RPMI 1640 (Invitrogen) containing 10 mM glucose and supplemented with 10% fetal bovine serum, streptomycin (100 μg/ml), penicillin (100 μg/ml), Na-pyruvate (1 mM), and 2-mercaptoethanol (50 μM). The cells were plated on polylysine-coated coverslips, transfected using Lipofectamine2000 (Invitrogen), and imaged 24–34 h later.

Solutions

The solution used for imaging contained 138 mM NaCl, 5.6 mM KCl, 1.2 mM $MgCl_2$, 2.6 mM $CaCl_2$, 3 mM D-glucose, and 5 mM HEPES (pH 7.4 with NaOH) at room temperature, except for exocytosis experiments (32°C). The solution for exocytosis experiments contained 10 mM glucose and was supplemented with 2 μM forskolin and 200 μM diazoxide, a K^+-ATP-channel opener that prevents glucose-dependent depolarization. Exocytosis was evoked by computer-controlled application of elevated K^+ (75 mM KCl equimolarly replacing NaCl in the standard imaging solution) through a pressurized glass pipette.

Constructs

To label granules, cells were transfected with plasmids encoding NPY-mCherry (Barg *et al.*, 2010; Gandasi *et al.*, 2015). Syntaxin-1 constructs are C-terminally tagged with EGFP and derived from the rat Syntaxin-1a-EGFP (Barg *et al.*, 2010; linker sequence: GVP-RARDPPVAT-EGFP) and Munc18 constructs from mouse Munc18-1-EGFP (open reading frame [ORF] from NM_001113569.1; Gandasi and Barg, 2014), all based on pEGFP-N1. Syntaxin 4-EGFP

contains the ORF from NM_031125.1 (rat) and Syntaxin-3-EGFP contains the ORF from NM_031124.1 (rat), both inserted into pEGFP-N1. The modifications of these vectors were done using PCR-based seamless cloning protocols using the Phusion DNA polymerase (Thermo-Fisher). The protein-coding DNA sequences of all constructs were confirmed by commercial sequencing (Eurofins Genomics). The backbones for all plasmids were derived from pEGFP-N1 (Clontech), with the exception of *Clostridium botulinum* neurotoxin C (BoNT-C, AB_745657.1, nucleotides 79–1424), which was coexpressed with NPY-mCherry from the bicistronic vector pIRES (Clontech). NPY-mCherry was cloned into the first slot (before the IRES site) and BoNT-C into the second slot of pIRES. As a control for these experiments, we used pIRES with NPY-mCherry in the first slot and the second slot empty.

Syntaxin-1 deletion mutants:

Stx1ΔNpep: aa 2–27 deleted

Stx1ΔHa: aa 28–62 deleted

Stx1ΔHb: aa 71–104 deleted

Stx1ΔHc: aa 111–144 deleted

Stx1ΔHab: aa 28–104 deleted

Stx1ΔHbc: aa 71–144 deleted

Stx1ΔHabc: aa 28–144 deleted

Stx1ΔHac: aa 28–62 and 111–144 deleted

Syntaxin-1/-4 hybrids:

Stx1Ha4: Stx1 with aa 30–64 replaced by stx4 aa 37–72.

Stx1Hb4: Stx1 with aa 65–108 replaced by stx4 aa 75–116.

Stx1Hc4: Stx1 with aa 110–160 replaced by stx4 aa 118–168.

Stx1Sn4: Stx1 with aa 183–246 replaced by stx4 aa 191–254.

Stx1Hab4: Stx1 with aa 30–108 replaced by stx4 aa 37–116.

Stx1Hbc4: Stx1 with aa 65–160 replaced by stx4 aa 75–168.

Stx1HcSn4: Stx1 with aa 110–246 replaced by stx4 aa 118–254.

Stx1Hac4: Stx1 with aa 30–64 and 110–160 replaced by stx4 aa 37–72 and 118–168, respectively.

Syntaxin-1 point mutations:

$Stx1^{SATTSS}$: aa 260–265 (KARRKK) changed to SATTSS

$Stx1^{txres}$: (BoNT-C resistant mutant) aa 252–255 KKAV changed to LIYF

$Stx1^{DEND}$: stx1 with mutations D231A E234A N236A D242A

$Stx1^{SS}$: stx1 with mutations A111S, I115S

$Stx1^{VM}$: stx1 with mutations A111V, I115M

$Stx4^{AI}$: stx1 with mutations V118A, M122I

Munc18-1 point mutations:

$Munc18^{EK}$: K46E, E59K mutations in rat munc18-1

Microscopy

Cells were imaged using a custom-built lens-type total internal reflection (TIRF) microscope based on an AxioObserver Z1 with a 100×/1.45 objective (Carl Zeiss). Excitation was from two DPSS lasers at 491 and 561 nm (Cobolt) passed through a cleanup filter (zet405/488/561/640×; Chroma) and controlled with an acousto-optical tunable filter (AA-Opto). Excitation and emission light were separated using a beamsplitter (ZT405/488/561/640rpc; Chroma). The emission light was chromatically separated onto separate areas of an EMCCD camera (Roper QuantEM 512SC) using an image splitter (Optical Insights) with a cutoff at 565 nm (565dcxr; Chroma) and emission filters (ET525/50m and 600/50m; Chroma). Scaling was 160 nm per pixel. For still images, the two color channels were acquired sequentially, first with cells exposed to 491 nm (1 mW) for 1 s (50 × 20 ms average), immediately followed by 561 nm (0.5 mW) for 100 ms. Movies were recorded with 100-ms exposures in stream mode (10 frames s^{-1}) and exciting simultaneously with 491 and 561 nm light. Alignment of the two color channels was corrected offline as previously described (Taraska *et al.*, 2003).

Image analysis

The fluorescence emitted by the cell (F) was calculated as the average pixel value in the footprint of the cell, corrected for out-of-cell background (bg). F was then normalized (F/F_0) to the first frame of the movie (F_0). All other measurements were specific for granules: granules that were well separated from other granules or the edge of the cell were identified, and an algorithm implemented as MetaMorph journal then read the average pixel fluorescence in 1) a central circle (c) of diameter 3 pixels (0.5 µm), 2) a surrounding annulus (a) with an outer diameter of 5 pixels (0.8 µm), and 3) an area not containing any cell as background (bg). The circle contains essentially all fluorescence originating from the granule site, plus the local background. The specific granule-associated fluorescence ΔF was calculated by subtracting the annulus value from that of the circle (ΔF = c – a). Local fluorescence unrelated to the granule site was calculated by subtracting the background from the annulus value (S = a – bg; Barg *et al.*, 2010). $\Delta F/S$ measures how well a protein binds to a granule: positive values indicate binding of syntaxin-EGFP to the granule site, negative values indicate exclusion. For syntaxin, the relation of ΔF over S follows a one-site binding model, $\Delta F = B_{max} \times S/(K_d + S)$ (Knowles *et al.*, 2010). For the relatively low expression levels in our experiments, the ratio ΔF/S is therefore proportional to the apparent affinity of the protein to the docking site. Note that ΔF is given as a per-pixel average for the entire 0.5-μm^{-2} circle, and $\Delta F/S$ values are therefore seemingly small. Assuming a cluster size of 50 nm, $\Delta F/S = 0.1$ corresponds to at least 20-fold enrichment in the cluster beneath a granule. Exocytosis events were found by eye as events with an obvious change in the fluorescence from the preexocytosis baseline followed by rapid loss of the signal.

Statistics

Experiments were repeated with at least three independent preparations. Data are presented as mean ± SEM unless otherwise stated, and number of cells is given in the text or within bar graphs. Statistical significance was tested using Student's t test for two-tailed paired or unpaired samples, as appropriate. Significant difference is indicated by asterisks (*$p < 0.05$, **$p < 0.01$, ***$p < 0.001$).

ACKNOWLEDGMENTS

We thank Frida Strömberg (Uppsala University) for assistance with some of the imaging experiments and Alenka Gucek and Per-Eric Lund for comments on the final version of the manuscript. The work was supported by the Swedish Science Council, the Diabetes Wellness Network Sweden, the Swedish Diabetes Society, the European Foundation for the Study of Diabetes, Hjärnfonden, Barndiabetesfonden, and the NovoNordisk-, Göran Gustafsson-, Family Ernfors-, Zetterlings-, and OE&E Johanssons-foundations. N.R.G. was supported by the European Foundation for the Study of Diabetes (EFSD) and the Swedish Society for Medical Research.

REFERENCES

Aoyagi K, Sugaya T, Umeda M, Yamamoto S, Terakawa S, Takahashi M (2005). The activation of exocytotic sites by the formation of phosphatidylinositol 4,5-bisphosphate microdomains at syntaxin clusters. J Biol Chem 280, 17346–17352.

Baker RW, Jeffrey PD, Zick M, Phillips BP, Wickner WT, Hughson FM (2015). A direct role for the Sec1/Munc18-family protein Vps33 as a template for SNARE assembly. Science 349, 1111–1114.

Barg S, Knowles MK, Chen X, Midorikawa M, Almers W (2010). Syntaxin clusters assemble reversibly at sites of secretory granules in live cells. Proc Natl Acad Sci USA 107, 20804–20809.

Bar-On D, Wolter S, van de Linde S, Heilemann M, Nudelman G, Nachliel E, Gutman M, Sauer M, Ashery U (2012). Super-resolution imaging reveals the internal architecture of nano-sized syntaxin clusters. J Biol Chem 287, 27158–27167.

Burkhardt P, Hattendorf DA, Weis WI, Fasshauer D (2008). Munc18a controls SNARE assembly through its interaction with the syntaxin N-peptide. EMBO J 27, 923–933.

Chen X, Lu J, Dulubova I, Rizo J (2008). NMR analysis of the closed conformation of syntaxin-1. J Biomol NMR 41, 43–54.

Colbert KN, Hattendorf DA, Weiss TM, Burkhardt P, Fasshauer D, Weis WI (2013). Syntaxin1a variants lacking an N-peptide or bearing the LE mutation bind to Munc18a in a closed conformation. Proc Natl Acad Sci 110, 12637–12642.

Dawidowski D, Cafiso DS (2013). Allosteric control of syntaxin 1a by Munc18-1: Characterization of the open and closed conformations of syntaxin. Biophys J 104, 1585–1594.

de Wit H, Cornelisse LN, Toonen RFG, Verhage M (2006). Docking of secretory vesicles is syntaxin dependent. PLoS One 1, e126.

Dulubova I, Sugita S, Hill S, Hosaka M, Fernandez I, Sudhof TC, Rizo J (1999). A conformational switch in syntaxin during exocytosis: role of munc18. EMBO J 18, 4372–4382.

Gandasi NR, Barg S (2014). Contact-induced clustering of syntaxin and munc18 docks secretory granules at the exocytosis site. Nat Commun 5, 399–407.

Gandasi NR, Vestö K, Helou M, Yin P, Saras J, Barg S (2015). Survey of red fluorescence proteins as markers for secretory granule exocytosis. PLoS One 10, e0127801.

Gandasi NR, Yin P, Omar-Hmeadi M, Ottosson Laakso E, Vikman P, Barg S (2018). Glucose-dependent granule docking limits insulin secretion and Is decreased in human type 2 diabetes. Cell Metab 27, 470–478.

Gulyas-Kovacs A, de Wit H, Milosevic I, Kochubey O, Toonen R, Klingauf J, Verhage M, Sorensen JB (2007). Munc18-1: sequential interactions with the fusion machinery stimulate vesicle docking and priming. J Neurosci 27, 8676–8686.

Han L, Jiang T, Han GA, Malintan NT, Xie L, Wang L, Tse FW, Gaisano HY, Collins BM, Meunier FA, *et al*. (2009). Rescue of Munc18-1 and -2 double knockdown reveals the essential functions of interaction between Munc18 and closed syntaxin in PC12 cells. Mol Biol Cell 20, 4962–4975.

Honigmann A, van den Bogaart G, Iraheta E, Jelger Risselada H, Milovanovic D, Mueller V, Müllar S, Diederichsen U, Fasshauer D, Grubmüller H, *et al*. (2013). Phosphatidylinositol 4,5-bisphosphate clusters act as molecular beacons for vesicle recruitment. Nat Struct Mol Biol 20, 679–686.

Hu S-H, Christie MP, Saez NJ, Latham CF, Jarrott R, Lua LHL, Collins BM, Martin JL (2011). Possible roles for Munc18-1 domain 3a and Syntaxin1 N-peptide and C-terminal anchor in SNARE complex formation. Proc Natl Acad Sci USA 108, 1040–1045.

Jakhanwal S, Lee C, Urlaub H, Jahn R (2017). An activated Q-SNARE/SM protein complex as a possible intermediate in SNARE assembly. EMBO J 36, 1788–1802.

Khvotchev M, Dulubova I, Sun J, Dai H, Rizo J, Südhof TC (2007). Dual modes of Munc18-1/SNARE interactions are coupled by functionally critical binding to syntaxin-1 N terminus. J Neurosci 27, 12147–12155.

Knowles MK, Barg S, Wan L, Midorikawa M, Chen X, Almers W (2010). Single secretory granules of live cells recruit syntaxin-1 and synaptosomal associated protein 25 (SNAP-25) in large copy numbers. Proc Natl Acad Sci USA 107, 20810–20815.

Kutlu B, Burdick D, Baxter D, Rasschaert J, Flamez D, Eizirik DL, Welsh N, Goodman N, Hood L (2009). Detailed transcriptome atlas of the pancreatic beta cell. BMC Med Genomics 2, 3.

Lang T (2007). SNARE proteins and "membrane rafts." J Physiol 585, 693–698.

Lang T, Bruns D, Wenzel D, Riedel D, Holroyd P, Thiele C, Jahn R (2001). SNAREs are concentrated in cholesterol-dependent clusters that define docking and fusion sites for exocytosis. EMBO J 20, 2202–2213.

Liang B, Kiessling V, Tamm L (2013). Prefusion structure of syntaxin-1A suggests pathway for folding into neuronal *trans*-SNARE complex fusion intermediate. Proc Natl Acad Sci USA 110, 19384–19389.

Margittai M, Widengren J, Schweinberger E, Schröder GF, Felekyan S, Haustein E, König M, Fasshauer D, Grubmüller H, Jahn R, Seidel CAM (2003). Single-molecule fluorescence resonance energy transfer reveals a dynamic equilibrium between closed and open conformations of syntaxin 1. Proc Natl Acad Sci USA 100, 15516–15521.

Milovanovic D, Honigmann A, Koike S, Göttfert F, Pähler G, Junius M, Müllar S, Diederichsen U, Janshoff A, Grubmüller H, *et al*. (2015). Hydrophobic mismatch sorts SNARE proteins into distinct membrane domains. Nat Commun 6, 5984.

Misura KM, Scheller RH, Weis WI (2000). Three-dimensional structure of the neuronal-Sec1-syntaxin 1a complex. Nature 404, 355–362.

Murray DH, Tamm LK (2009). Clustering of syntaxin-1A in model membranes is modulated by phosphatidylinositol 4,5-bisphosphate and cholesterol. Biochemistry 48, 4617–4625.

Murray DH, Tamm LK (2011). Molecular mechanism of cholesterol- and polyphosphoinositide-mediated syntaxin clustering. Biochemistry 50, 9014–9022.

Ohara-Imaizumi M, Fujiwara T, Nakamichi Y, Okamura T, Akimoto Y, Kawai J, Matsushima S, Kawakami H, Watanabe T, Akagawa K, Nagamatsu S (2007). Imaging analysis reveals mechanistic differences between first- and second-phase insulin exocytosis. J Cell Biol 177, 695–705.

Ohara-Imaizumi M, Nishiwaki C, Kikuta T, Kumakura K, Nakamichi Y, Nagamatsu S (2004). Site of docking and fusion of insulin secretory granules in live MIN6 beta cells analyzed by TAT-conjugated anti-syntaxin 1 antibody and total internal reflection fluorescence microscopy. J Biol Chem 279, 8403–8408.

Park S, Bin NR, Michael Rajah M, Kim B, Chou TC, Kang SY, Sugita K, Parsaud L, Smith M, Monnier PP, *et al*. (2016). Conformational states of syntaxin-1 govern the necessity of N-peptide binding in exocytosis of PC12 cells and Caenorhabditis elegans. Mol Biol Cell 27, 669–685.

Peng R, Gallwitz D (2002). Sly1 protein bound to Golgi syntaxin Sed5p allows assembly and contributes to specificity of SNARE fusion complexes. J Cell Biol 157, 645–655.

Pertsinidis A, Mukherjee K, Sharma M, Pang ZP, Park SR, Zhang Y, Brunger AT, Sudhof TC, Chu S (2013). Ultrahigh-resolution imaging reveals formation of neuronal SNARE/Munc18 complexes in situ. Proc Natl Acad Sci USA 110, E2812–E2820.

Rathore SS, Bend EG, Yu H, Hammarlund M, Jorgensen EM, Shen J (2010). Syntaxin N-terminal peptide motif is an initiation factor for the assembly of the SNARE-Sec1/Munc18 membrane fusion complex. Proc Natl Acad Sci USA 107, 22399–22406.

Schiavo G, Shone CC, Bennett MK, Scheller RH, Montecucco C (1995). Botulinum neurotoxin type C cleaves a single Lys-Ala bond within the carboxyl-terminal region of syntaxins. J Biol Chem 270, 10566–10570.

Schütz D, Zilly F, Lang T, Jahn R, Bruns D (2005). A dual function for Munc-18 in exocytosis of PC12 cells. Eur J Neurosci 21, 2419–2432.

Shen J, Rathore SS, Khandan L, Rothman JE (2010). SNARE bundle and syntaxin N-peptide constitute a minimal complement for Munc18-1 activation of membrane fusion. J Cell Biol 190, 55–63.

Shen J, Tareste DC, Paumet F, Rothman JE, Melia TJ (2007). Selective activation of cognate SNAREpins by Sec1/Munc18 proteins. Cell 128, 183–195.

Shi L, Kummel D, Coleman J, Melia TJ, Giraudo CG (2011). Dual roles of Munc18-1 rely on distinct binding modes of the central cavity with Stx1A and SNARE complex. Mol Biol Cell 22, 4150–4160.

Sieber JJ, Willig KI, Heintzmann R, Hell SW, Lang T (2006). The SNARE motif is essential for the formation of syntaxin clusters in the plasma membrane. Biophys J 90, 2843–2851.

Sieber JJ, Willig KI, Kutzner C, Gerding-Reimers C, Harke B, Donnert G, Rammner B, Eggeling C, Hell SW, Grubmüller H, *et al*. (2007). Anatomy and dynamics of a supramolecular membrane protein cluster. Science 317, 1072–1076.

Sollner T, Bennett MK, Whiteheart SW, Scheller RH, Rothman JE (1993). A protein assembly-disassembly pathway in vitro that may correspond to sequential steps of synaptic vesicle docking, activation, and fusion. Cell 75, 409–418.

Sutton RB, Fasshauer D, Jahn R, Brunger AT (1998). Crystal structure of a SNARE complex involved in synaptic exocytosis at 2.4 A resolution. Nature 395, 347–353.

Taraska JW, Perrais D, Ohara-Imaizumi M, Nagamatsu S, Almers W (2003). Secretory granules are recaptured largely intact after stimulated exocytosis in cultured endocrine cells. Proc Natl Acad Sci USA 100, 2070–2075.

van den Bogaart G, Meyenberg K, Risselada HJ, Amin H, Willig KI, Hubrich BE, Dier M, Hell SW, Grubmüller H, Diederichsen U, *et al.* (2011). Membrane protein sequestering by ionic protein-lipid interactions. Nature 479, 552–555.

Voets T, Toonen RF, Brian EC, de Wit H, Moser T, Rettig J, Sudhof TC, Neher E, Verhage M (2001). Munc18-1 promotes large dense-core vesicle docking. Neuron 31, 581–591.

Weimbs T, Low SH, Chapin SJ, Mostov KE, Bucher P, Hofmann K (1997). A conserved domain is present in different families of vesicular fusion proteins: a new superfamily. Proc Natl Acad Sci USA 94, 3046–3051.

Yang X, Wang S, Sheng Y, Zhang M, Zou W, Wu L, Kang L, Rizo J, Zhang R, Xu T, *et al.* (2015). Syntaxin opening by the MUN domain underlies the function of Munc13 in synaptic-vesicle priming. Nat Struct Mol Biol 22, 547–554.

Zhou P, Pang ZP, Yang X, Zhang Y, Rosenmund C, Bacaj T, Südhof TC, Sudhof TC (2013). Syntaxin-1 N-peptide and Habc-domain perform distinct essential functions in synaptic vesicle fusion. EMBO J 32, 159–171.

Zilly FE, Sørensen JB, Jahn R, Lang T (2006). Munc18-bound syntaxin readily forms SNARE complexes with synaptobrevin in native plasma membranes. PLoS Biol 4, e330.